Human Molecular Genetics, 2004, Vol. 13, No. 12 **1225–1240**
DOI: 10.1093/hmg/ddh140
Advance Access published on April 28, 2004

Gene expression profiles of transcripts in amyloid precursor protein transgenic mice: up-regulation of mitochondrial metabolism and apoptotic genes is an early cellular change in Alzheimer's disease

P. Hemachandra Reddy[1,*], Shannon McWeeney[3,4], Byung S. Park[3,4], Maria Manczak[1], Ramana V. Gutala[1], Dara Partovi[1], Youngsin Jung[1], Vincent Yau[3], Robert Searles[2], Motomi Mori[3,4] and Joseph Quinn[5,6]

[1]Neurogenetics Laboratory, Neurological Sciences Institute, [2]Spotted Microarray Core, Gene Microarray Shared Resource, Oregon Health and Science University, 505 NW 185th Avenue, Beaverton, OR 97006, USA, [3]Bioinformatics and Biostatistics Core, Gene Microarray Shared Resource, [4]Division of Biostatistics, Department of Public Health and Preventive Medicine, Oregon Health and Science University, 3181 SW Sam Jackson Park Rd, Portland, OR 97239, USA, [5]Department of Neurology, Portland Veteran's Affairs Medical Center and [6]Department of Neurology, Oregon Health and Science University, 3181 SW Sam Jackson Park Rd, Portland, OR 97201, USA

Received January 23, 2004; Revised and Accepted April 15, 2004

Alzheimer's disease (AD) is a progressive neurodegenerative disease characterized by the impairment of cognitive functions and by beta amyloid (Aβ) plaques in the cerebral cortex and the hippocampus. Our objective was to determine genes that are critical for cellular changes in AD progression, with particular emphasis on changes early in disease progression. We investigated an established amyloid precursor protein (APP) transgenic mouse model (the Tg2576 mouse model) for gene expression profiles at three stages of disease progression: long before (2 months of age), immediately before (5 months) and after (18 months) the appearance of Aβ plaques. Using cDNA microarray techniques, we measured mRNA levels in 11 283 cDNA clones from the cerebral cortex of Tg2576 mice and age-matched wild-type (WT) mice at each of the three time points. This gene expression analysis revealed that the genes related to mitochondrial energy metabolism and apoptosis were up-regulated in 2-month-old Tg2576 mice and that the same genes were up-regulated at 5 and 18 months of age. These microarray results were confirmed using northern blot analysis. Results from *in situ* hybridization of mitochondrial genes—ATPase-6, heat-shock protein 86 and programmed cell death gene 8—suggest that the granule cells of the hippocampal dentate gyrus and the pyramidal neurons in the hippocampus and the cerebral cortex are up-regulated in Tg2576 mice compared with WT mice. Results from double-labeling *in situ* hybridization suggest that in Tg2576 mice only selective, over-expressed neurons with the mitochondrial gene ATPase-6 undergo oxidative damage. These results, therefore, suggest that mitochondrial energy metabolism is impaired by the expression of mutant APP and/or Aβ, and that the up-regulation of mitochondrial genes is a compensatory response. These findings have important implications for understanding the mechanism of Aβ toxicity in AD and for developing therapeutic strategies for AD.

INTRODUCTION

Alzheimer's disease (AD) is a complex and progressive neurodegenerative disorder characterized clinically by memory loss, impairment of other cognitive functions and changes in behavior and personality. The AD pathology is characterized by beta amyloid (Aβ) plaques, neurofibrillary tangles, neuronal degeneration and synaptic changes (1–4). The pathogenesis

*To whom correspondence should be addressed at: Neurogenetics Laboratory, Neurological Sciences Institute, Oregon Health and Science University, 505 NW 185th Avenue, Beaverton, OR 97006, USA. Tel: +1 5034182625; Fax: +1 5034182501; Email: reddyh@ohsu.edu

 © *Oxford University Press 2004; all rights reserved*

Downloaded from https://academic.oup.com/hmg/article/13/12/1225/587912 by guest on 16 August 2022

of AD has not been established with certainty, but abnormalities in the processing of amyloid precursor protein (APP) have been implicated. Specifically, mutations in APP have been found to be sufficient to produce the clinical and pathologic features of autosomal dominant AD (1–3).

While more common sporadic forms of AD are clearly not associated with such mutations, the 'amyloid hypothesis' holds that both hereditary and sporadic forms of AD are due to neurotoxic effects of Aβ (1). This hypothesis remains controversial, however, for a number of reasons, including the weak correlation between the amyloid burden and the severity of dementia in patients with AD (5). The amyloid hypothesis has also been strained by the discordance of results between cell culture and animal studies concerning Aβ toxicity. Cytotoxicity of Aβ has been demonstrated *in vitro* (6–8), and the injection of Aβ peptides into intact animal brains has shown inconsistency in neuronal loss (9,10). The over-expression of APP and Aβ in transgenic mice lines has also failed to produce neuronal death in AD, despite the presence of neuritic plaques in some of these transgenic lines (11–17). However, some of these transgenic lines show signs of neuronal dysfunction in the form of hippocampal-dependent, spatial memory impairments (18–21).

The mechanisms by which APP over-expression produces neuronal dysfunction remain unclear, with hypotheses ranging from synaptotoxic (22,23) to vasoactive (24,25) effects of Aβ species. Further, in AD progression, the ordering of cellular events due to the over-expression of mutant APP is not clear. Recently, it has been reported that the effects of soluble and insoluble Aβ may lead to AD progression (4). While Aβ is hypothesized to play a role in AD pathogenesis, several questions relating to AD progression need to be addressed, including: what cellular changes occur early in the progression of AD—even before AD pathological features manifest? How does a mutant APP or Aβ cause cellular changes? Answers to these questions would help in the development of early detectable biomarkers for AD, and this information could be useful particularly in the development of therapeutic strategies to delay or even to arrest the progression of AD caused by mutant APP and/or Aβ peptides.

Microarray-based gene expression studies permit an open-ended approach to answer the question of how neurons may be altered functionally by APP and Aβ over-expressions. The major objective of our research was to determine cellular changes in the cerebral cortex throughout the Tg2576 mouse life cycle. We used cDNA microarray techniques to identify the genes that are critical for early cellular changes in the development and progression of AD in an APP mouse model. We measured the expression of 11 283 embryonically expressed cDNA clones in the cerebral cortex of wild-type (WT) mice and Tg2576 mice at three stages of disease progression: long before (2 months old), immediately before (5 months old) and after (18 months old) the appearance of amyloid pathology and cognitive impairment.

Comparing gene expressions in the brains of Tg2576 mice (11) and WT mice, we noted a consistent increase in mitochondrial gene expression in the APP over-expressing animals, even at ages before Aβ plaques were evident. This increase in mitochondrial gene expression was evident throughout the Tg2576 mouse life cycle and was influenced by a concomitant up-regulation of genes associated with oxidative damage, suggesting that the change in mitochondrial gene expression is either deleterious itself or represents a compensatory response to an APP-induced mitochondrial dysfunction. The regional distribution of this change in gene expression was also examined with *in situ* hybridization and immuno-histochemistry that localized differentially expressed RNA and protein in brain tissue from Tg2576 mice.

RESULTS

Gene expression differences in APP mice versus WT mice

Table 1 summarizes the global screening of our gene expression analysis of cerebral cortex brain specimens from Tg2576 mice and age-matched WT mice. The number of putatively differentially expressed genes between Tg2576 mice and WT mice increased with age, with the largest increase at 18 months (Fig. 1).

Our comparative gene expression analysis of Tg2576 mice and WT mice at the cut-off ratio of >2 mRNA fold change revealed 83 putatively up-regulated genes and 26 putatively down-regulated genes. In 5-month-old Tg2576 mice, we found 54 genes up-regulated and 30 genes down-regulated, and these numbers greatly increased in 18-month-old Tg2576 mice, with 108 genes up-regulated and 149 genes down-regulated (Table 1).

In addition, in 2-month-old mice, we found that most of the differentially expressed genes were related to mitochondrial energy metabolism, particularly genes related to oxidative phosphorylation (OXPHOS) and also to apoptosis. The same OXPHOS genes were still up-regulated in 5- and 18-month-old Tg2576 mice. Details of differentially expressed genes (up- and down-regulated) at three different stages of AD progression are given in Supplementary Material (Table S1).

Validation of microarray results—northern blot analysis of differentially expressed genes

To confirm our microarray results, we used northern blot analysis to investigate the RNA expression of 18 up-regulated genes (mainly mitochondrial-encoded OXPHOS genes) in the cerebral cortex (affected in AD) and the cerebellum (unaffected in AD) of Tg2576 mice and age-matched WT mice at the three stages of AD progression. The northern blot data from the cerebral cortex agreed with our original cDNA microarray results (Fig. 2 and Table 2), independently validating the conclusions drawn from our microarray studies.

To determine whether increased mitochondrial mRNA expressions are confined to the cerebral cortex and not to the cerebellum, we conducted northern blot analysis using RNA from cerebellar tissues from Tg2576 mice and age-matched WT mice at the three stages of AD progression. In these cerebellar tissues, we did not find any differences in mRNA expression between Tg2576 mice and WT mice at any of the three stages (Table 2 and Supplementary Material, Fig. S2), suggesting that up-regulated gene expressions in Tg2576 mice are related to AD.

Downloaded from https://academic.oup.com/hmg/article/13/12/1225/587912 by guest on 16 August 2022

Table 1. Summary of gene expression analysis of Tg2576 mice and WT mice at three stages of disease progression

	2-Month-old mice (long before amyloid pathology)	5-Month-old mice (immediately before amyloid pathology)	18-Month-old mice (after amyloid pathology and cognitive impairment)
Total cDNA clones screened (NIA mouse cDNA library)	11 283	11 283	11 283
Genes with detectable expressions (above threshold cut-off)	5243	5630	5956
Differential expression of known genes at the cut-off ratio >2 fold	Total genes $n = 109$, up-regulated genes $n = 83$, down-regulated genes $n = 26$	Total genes $n = 84$, up-regulated genes $n = 54$, down-regulated genes $n = 30$	Total genes $n = 257$, up-regulated genes $n = 108$, down-regulated genes $n = 149$
Cellular pathways of differentially regulated genes	Mitochondrial energy metabolism, apoptosis and cytoskeletal	Mitochondrial energy metabolism, apoptosis and cytoskeletal	Mitochondrial energy metabolism, apoptosis, cytoskeletal, transcription factors, cell-cycle development and regulation, signal transduction and autoimmunity

Details of genes known to be differentially expressed, at three different stages of AD progression in APP mice, are given in Supplementary Material (Table S1). Gene expression data are available at www.ohsu.edu/gmsr/bbc/miame.

In situ hybridization of mitochondrial, apoptotic and heat-shock protein genes in the brain specimens of Tg2576 mice and WT mice

To determine the localization of mitochondrial gene expressions and to understand the differentially expressed population of neurons, using *in situ* hybridization techniques, we studied ATPase-6 in complex V of OXPHOS, programmed cell death gene 8 and heat-shock protein 86 from the brain specimens of 7-month-old Tg2576 mice and age-matched WT mice. Our *in situ* hybridization analysis revealed that ATPase-6 (Fig. 3A–D), programmed cell death gene 8 (Fig. 4A–D) and heat-shock protein 86 (Fig. 5A–D) levels were high in the brain sections of the Tg2576 mice compared with those of the age-matched WT mice. Further, these over-expressed mRNAs were found to be localized in the cytoplasm of pyramidal neurons of the hippocampus and the cerebral cortex, suggesting that the over-expression of ATPase-6, programmed cell death gene 8 and heat-shock protein 86 are associated with Aβ toxicity in Tg2576 mice. We also observed that granule cells in the dentate gyrus of the hippocampus were over-expressed for all of the genes examined in Tg2576 mice, suggesting that dentate gyrus is affected more severely than any other region in the hippocampus, which may be due to toxicity of APP over-expression in Tg2576 mice. We did not observe the over-expression of ATPase-6 in complex V of OXPHOS (Fig. 3E and F), programmed cell death gene 8 (Fig. 4E and F) and heat-shock protein 86 (Fig. 5E and F) in the striatum, the less plaque-developed tissue of Tg2576 mice, suggesting that the over-expression of mitochondrial genes is confined to plaque-developed regions in Tg2576 mice.

Immunofluorescence analysis of oxidative damage in the brain specimens of Tg2576 mice and WT mice

To determine the relationship between mitochondrial gene up-regulation and oxidative damage, we also studied 8-hydroxyguanosine (8-OHG), a marker for oxidative damage in 7-month-old Tg2576 mice ($n = 5$) and age-matched WT mice ($n = 5$) brain specimens. Our immunofluorescence analysis of oxidative damage marker 8-OHG revealed an increased expression of 8-OHG in the hippocampus and the cerebral cortex sections from these mice (Fig. 6B and D) compared with those from age-matched WT mice (Fig. 6A and C), suggesting oxidative damage in Tg2576 mice.

Double-labeling of mitochondrial gene, ATPase-6 and oxidative damage marker 8-OHG in Tg2576 mice and WT mice

To determine whether neurons showing increased ATPase-6 are vulnerable to oxidative damage, we conducted double-labeling, which is a combination of *in situ* hybridization and immunofluorescence analyses. Our double-labeling in *in situ* hybridization of the mitochondrial gene ATPase-6 and the immunofluorescence analysis of 8-OHG (green, Fig. 7A) and 8-OHG (red, Fig. 7B) revealed that in the brain sections from 7-month-old Tg2576 mice, over-expressed neurons with ATPase-6 showed positive immunoreactivity for 8-OHG [overlaid with green (ATPase-6) and red (8-OHG); Fig. 7C].

DISCUSSION

In the present study, we studied the gene expression profiles of transcripts from both Tg2576 mice and age-matched WT mice. Our genome-wide survey of gene expression points to changes in mitochondrial and apoptosis-associated genes as the most prominent gene expression consequence of APP over-expression in the Tg2576 mouse. We verified these changes in gene expression with northern blot analysis. We conclude that APP over-expression promotes both mitochondrial gene up-regulation and oxidative damage in these experimental systems, and we hypothesize that these mechanisms are relevant to human AD.

Downloaded from https://academic.oup.com/hmg/article/13/12/1225/587912 by guest on 16 August 2022

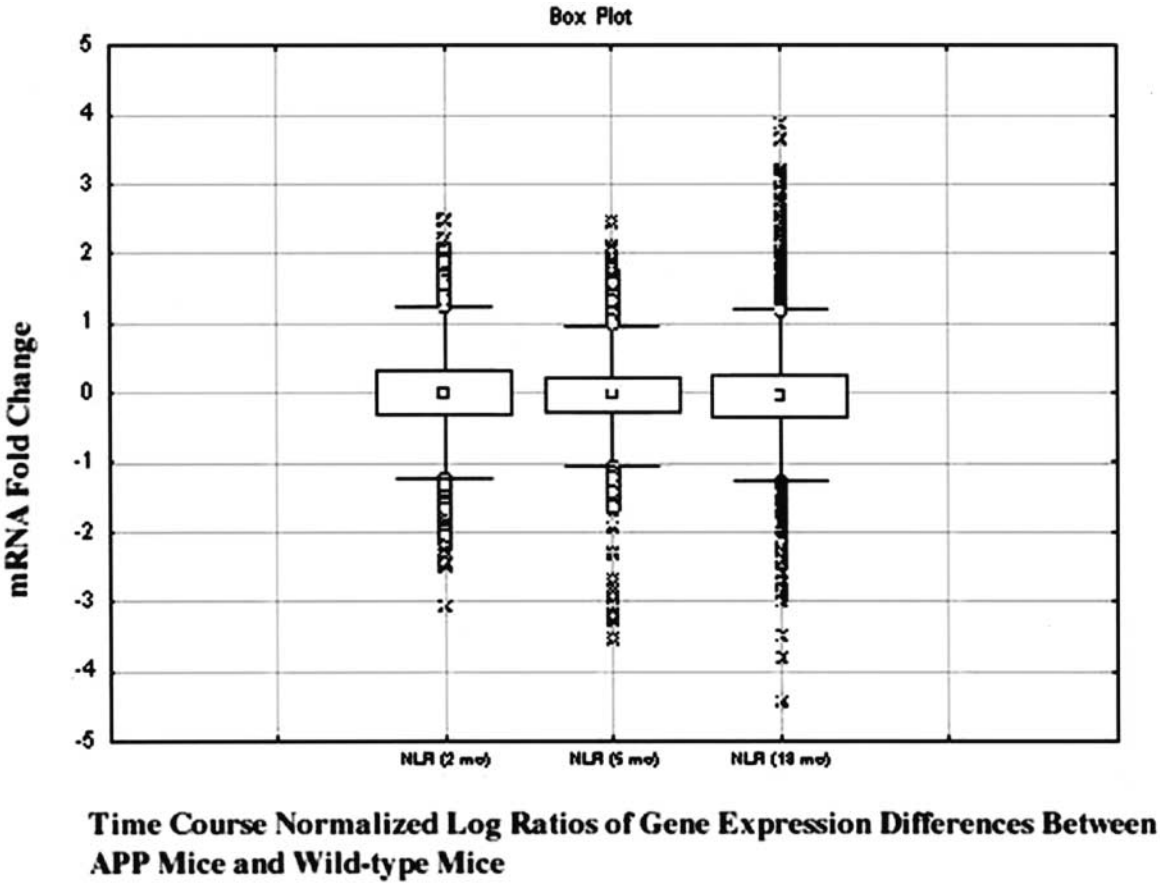

Figure 1. Side-by-side box plots of the NLR of gene expressions at three stages of disease progression for Tg2576 mice and age-matched WT mice. The box plot shows the middle 50% of the data as a box and highlights various features of the distribution, including the upper 25%, the lower 25% and outliers. Distributions of NLR for each stage were about the same (the middle 50%), but the distributions of the NLR of 18-month-old mice show more variations and extreme values.

Differential expression of genes in APP mice—increased mRNA expressions

In our genome-wide screen of Tg2576 mice, we found that the majority of up-regulated genes were associated with mitochondrial energy metabolism, cytoskeletal, ubiquitins and apoptotic cell death. It is interesting to note that the increased number of mRNA in mitochondrial-encoded genes were responsible for complexes I, III–V of OXPHOS in the cell metabolism of 2-month-old Tg2576 mice. This increased mRNA expression of mitochondrial-encoded genes was also up-regulated in 5- and 18-month-old Tg2576 mice compared with those in age-matched WT mice.

We did not observe an up-regulation of nuclear-encoded genes related to energy metabolism in any sections from Tg2576 mice at the three stages of disease progression, suggesting that mutant APP or soluble Aβ may target mitochondrial-encoded genes in Tg2576 mice.

We verified the up-regulated mitochondrial genes in the cerebral cortex by northern blot analysis. Overall, both northern blot and microarray methods showed increased mitochondrial gene expression throughout the 2- to 18-month interval. However, we found mitochondrial gene expression differences between northern blot and microarray results. The possible reasons for mRNA differences between these two methods are the amount of RNA used and the sensitivity of these techniques to detect mRNA.

Our northern blot analysis of the cerebral cortex and the cerebellum of Tg2576 mice, in comparison with WT mice, suggests that increased mitochondrial gene expression is confined to cerebral cortex. It has been reported that a mutant human APP transgene is over-expressed in the cerebellum, the cerebral cortex and the hippocampus (26,27) of Tg2576 mice, but the Aβ deposition is restricted to the cortex and the hippocampus. Despite the mutant human APP over-expression in the cerebellum, cortex and hippocampus of Tg2576 mice (27), we found an up-regulation of mitochondrial genes in the cortex and the hippocampus and not in the cerebellum, suggesting that increased mitochondrial gene expression is relevant to AD progression in Tg2576 mice.

In our studies, northern blot analysis also revealed an increase of mRNA for several mitochondrial genes, including NADH subunit 2, NADH subunit 3, cytochrome oxidase 2, cytochrome oxidase 3 and nexin 14 in non-transgenic WT mice, suggesting that aging is an important factor for age-related AD progression. This possibility in turn suggests that the over-expression of the mutant APP transgene may provoke changes similar to those that occur normally with

Downloaded from https://academic.oup.com/hmg/article/13/12/1225/587912 by guest on 16 August 2022

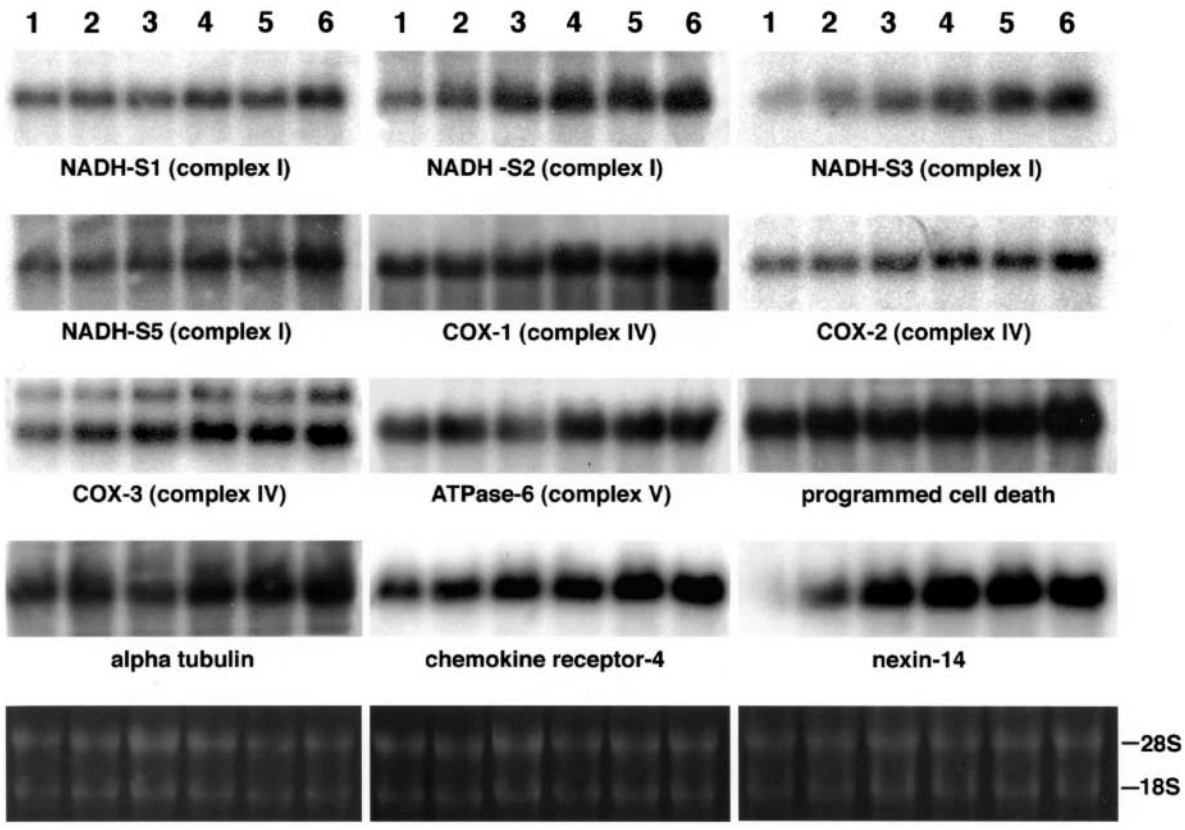

Figure 2. Northern blot analysis of a few representative, up-regulated genes from brain slices from APP mice and age-matched WT mice. Lanes of RNA sources: lanes 1, 2 and 3 represent 2-, 5- and 18-month-old WT mice, respectively, and lanes 4, 5 and 6 represent 2-, 5- and 18-month-old Tg2576 mice, respectively. An amount of 5 μg of RNA was loaded in each lane. The bottom panel represents RNA bands in formamide/agarose gel for equal loading.

aging. Some genes up-regulate in non-transgenic mice in response to age-related Aβ aggregation, thus effectively preventing plaque formation. However, in transgenic mice, this compensatory change is maximal owing to very early transgene-induced Aβ aggregation, thus possibly effectively preventing plaque formation and cognitive decline for a time but ultimately 'giving out'.

The genes in Table 2 are demarcated by mitochondrial and/or oxidoreductase activity, as well as those involved in apoptosis (28–31) are likely candidates for involvement in an oxidative stress pathway. We also found an increased mRNA expression of heat-shock proteins 86 and 70, and several proteosome-complex-related genes such as ubiquitin B and ubiquitin C. The up-regulation of heat-shock proteins and proteosome-complex-related genes suggests that in Tg2576 mice there may be a strong neuro-protective mechanism that is likely toxicity generated by mutant APP or Aβ. Heat-shock proteins serve as molecular chaperones to protect cells from various forms of stress (32). Given the broad cytoprotective properties of the heat-shock response, there is increasing interest in discovering and developing pharmacological agents capable of inducing the heat-shock response.

The proteosome is a multi-catalytic complex involved in the degradation of poly-ubiquitinated proteins. It has been observed that soluble Aβ binds to proteosome genes and interacts with the inner catalytic compartment of enzymes, triggering proteosomal complexes to protect the ubiquinated proteosomal substrates (33). The same study suggests that Aβ prevents the degradation of ubiquitin-dependent proteins (33). To compensate for the toxicity generated by intracellular Aβ, proteosome genes and heat-shock proteins may become up-regulated in Tg2576 mice.

In our study, cytoskeletal proteins—including alpha tubulins, beta tubulins, actins (cytoplasmic), actin-like cytoskeletal genes, keratin and integrin beta—were up-regulated in APP mice, suggesting that in Tg2576 mice the cytoskeleton is altered, probably due to Aβ toxicity.

Decreased mRNA expressions

We found that several AD-associated genes, such as the activity-regulated cytoskeletal-associated protein, proteosome 26S subunit, S100 calcium binding protein, synapsin 1 and cadherin 1 were down-regulated in 2-month-old Tg2576 mice. We found a similar trend for 5- and 18-month-old Tg2576 mice compared with age-matched WT mice (Supplementary Material, Table S1). We also found a large number of genes that are related to multiple cellular pathways to be down-regulated in 18-month-old Tg2576 mice.

It is interesting to note that the differential expression of genes observed in 2- and 5-month-old Tg2576 mice (before Aβ plaque formation) suggested that mutant APP and

Downloaded from https://academic.oup.com/hmg/article/13/12/1225/587912 by guest on 16 August 2022

Downloaded from https://academic.oup.com/hmg/article/13/12/1225/587912 by guest on 16 August 2022

Table 2. Putatively up-regulated genes in Tg2576 mice compared with WT mice at 2, 5 and 18 months of age. The genes listed have been confirmed by northern blot analysis. Entries in italics are genes that were examined by northern blot analysis but were not on the cDNA chip

Gene description	Northern data in the cortex — Tg2576 mice/WT mice			Northern data in the cerebellum — Tg2576 mice/WT mice			Microarray data in the cortex		
	2 months	5 months	18 months	2 months	5 months	18 months	2 months	5 months	18 months
NADH subunit 1 complex I (mt. genome, nucleotide pos.3333–3391 for northern probe)	*1.67*	*1.67*	*1.86*	0.91	1.1	1.06			
NADH subunit 2 complex I (mt. genome, nucleotide pos. 4052–4137 for northern probe)	*2.87*	*2.31*	*2.10*	0.95	1.02	1.09			
NADH subunit 3 complex I (mt. genome, nucleotide pos. 9544–9621 for northern probe)	*2.73*	*1.84*	*1.44*	1.08	0.96	1.0			
NADH subunit 4 complex I (BG065291)	1.99	1.85	2.25	1.00	0.96	0.99	2.37	2.01	3.22
NADH subunit 5 complex I (BG078136)	2.25	2.50	2.00	0.89	0.88	1.00	2.41	2.76	2.28
NADH subunit 6 complex I (mt. genome, nucleotide pos. 13643–13722 for northern probe)	*1.85*	*2.05*	*1.85*	1.12	0.96	0.96			
Cytochrome-*b* complex III (BG064785)	1.73	2.00	2.13	0.95	1.14	0.97	3.13	3.15	4.06
Cytochrome-*c*-oxidase 1 complex IV (BG085515)	1.70	1.74	1.66	0.98	0.98	1.04	3.45	3.53	2.60
Cytochrome-*c*-oxidase subunit 2 (BI076595)	2.92	2.16	1.87	1.08	0.97	1.02	2.41	2.46	1.73
Cytochrome-c-oxidase subunit 3 (mt. genome, nucleotide pos. 8890–8969 for northern probe)	2.09	1.17	1.58	0.88	1.02	1.01			
ATPase 6 complex V (BG086028)	1.94	2.11	2.99	0.96	1.04	1.02	2.73	3.81	2.32
CXCR 4 (BG063365)	2.82	2.60	2.72	0.91	0.92	1.10	2.72	1.93	2.99
Programmed cell death gene 8 (C85471)	1.80	1.47	1.56	0.97	0.82	1.01	2.57	2.43	6.19
Nexin 14 (AW538640)	3.11	2.57	1.75				3.26	2.40	3.18
Tripeptidyl peptidase (BG064856)	0.97	2.63	2.76	0.80	1.02	0.98	3.05	3.32	4.23
Heat-shock protein 86 (BG064775)	3.36	2.61	1.96	0.88	1.08	1.08	2.10	1.61	3.04
Alpha tubulin (BG064838)	1.35	1.20	2.36	0.95	0.99	1.01	1.48	2.21	1.63

Northern blot analysis verified the representative polypeptide genes from each complex of the OXPHOS of electron transport chains and from other top-most up-regulated genes in our gene expression analysis.

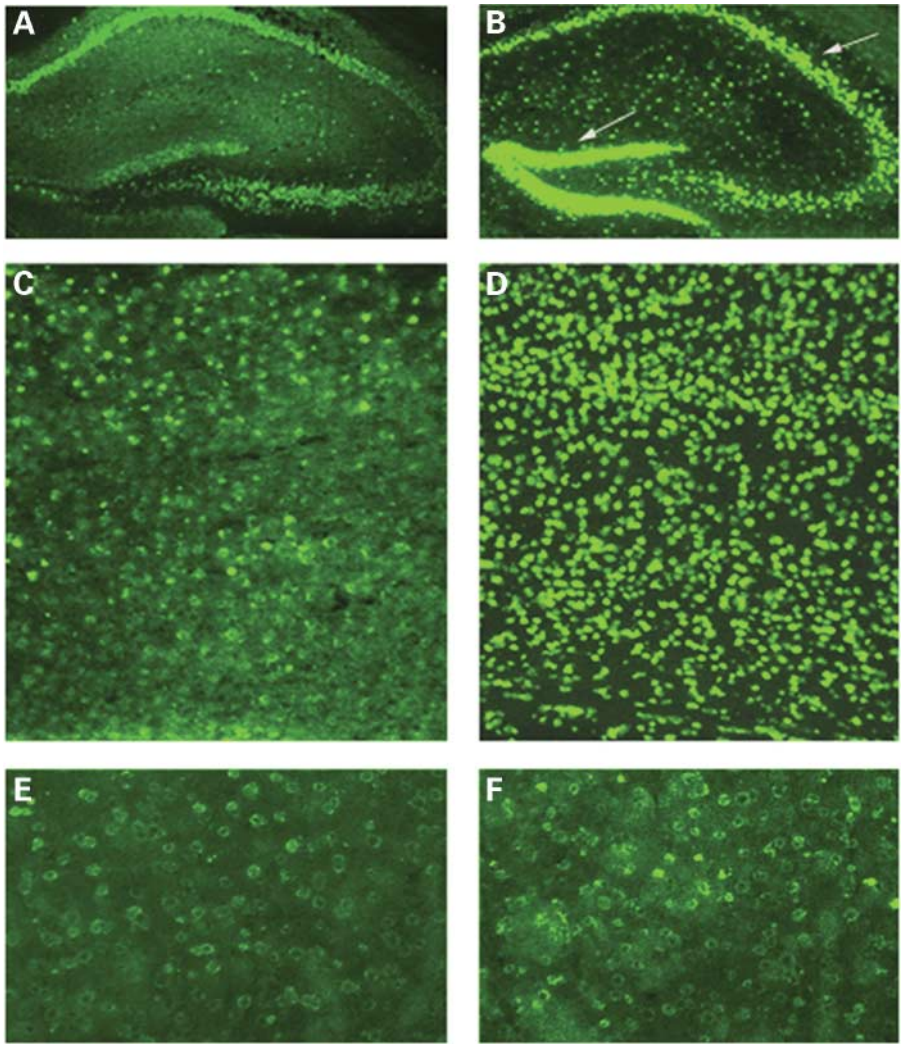

Figure 3. *In situ* hybridization of the mitochondrial gene ATPase-6. Increased mRNA expression of ATP-6 in green fluorescence is shown in the hippocampus (**A**) and the cerebral cortex (**C**) of age-matched WT mice, compared with sections from the hippocampus (**B**) and the cerebral cortex (**D**) in sections from 7-month-old Tg2576 mice. mRNA expression is unchanged for the striatum between Tg2576 mice (**F**) and age-matched WT mice (**E**). Arrows indicate the over-expression of ATPase-6 in dentate gyrus, CA1–CA3 regions and all layers of the cerebral cortex. Hippocampal sections were photographed at 40× the original magnification, and the cerebral cortex and striatal sections were photographed at 100× the original magnification.

soluble Aβ may be responsible for this differential expression of genes. Further, we found a large number of genes differentially expressed in 18-month-old Tg2576 mice, suggesting that in the late stages of AD, genes related to multiple cellular pathways are altered in agreement with a recent study by Loring *et al.* (34).

Gene expression differences in APP transgenic mice

Differential expression of mitochondrial genes in the present study was not reported previously in a study of gene expression in Tg2576 mice, which also used microarray methods (35). In addition, in another gene expression study of APP + PS1 transgenic mice at 18 months of age (36), the investigators found a reduced expression of several genes essential for long-term potentiation and memory formation but no change related to mitochondrial gene expression. The previous studies differed from the present one in the portion of brain tissue examined (they studied the hippocampus), the stage of disease progression, the specific microarray methodology used (the prior study used an oligonucleotide-based Affymetrics gene expression system) and the representation of genes in the microarray. The brain region studied may account for some of our differing results. However, our *in situ* hybridization and immuno-histochemistry results suggest that the mitochondrial, oxidative damage and apoptotic cell death genes that we identified are expressed differentially in both the hippocampus and the cerebral cortex.

Metabolic changes in APP mice and in AD patients

Our gene expression findings are consistent with those from other studies on Tg2576 mice—studies that reported increased levels of both oxidative damage (37,38) and mitochondrial

Downloaded from https://academic.oup.com/hmg/article/13/12/1225/587912 by guest on 16 August 2022

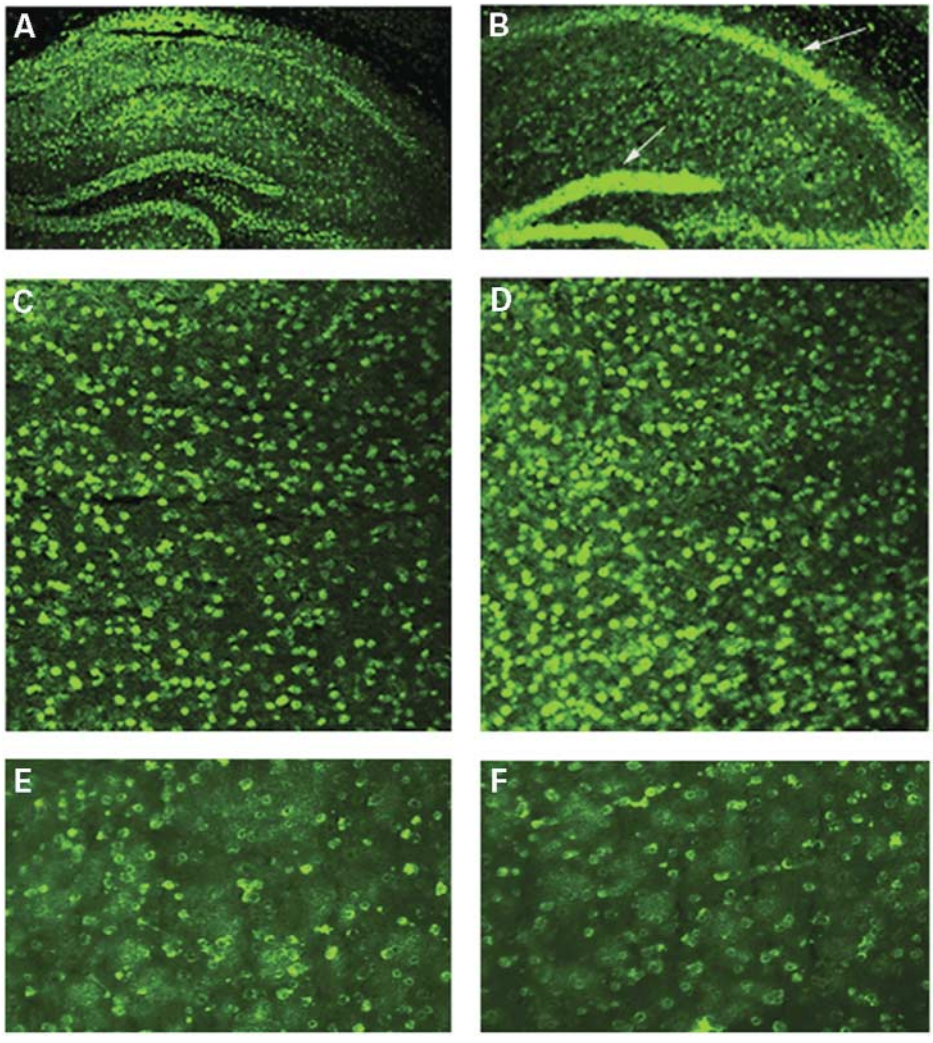

Figure 4. *In situ* hybridization of programmed cell death gene 8. Increased mRNA expression of programmed cell death gene 8 in green fluorescence is shown in the hippocampus (**A**) and the cerebral cortex (**C**) from age-matched WT mouse compared with sections from the hippocampus (**B**) and the cerebral cortex (**D**) sections from 7-month-old Tg2576 mice. mRNA expression is unchanged for the striatum between Tg2576 mice (**F**) and age-matched WT mice (**E**). Arrows indicate the over-expressions of programmed cell death gene 8 in dentate gyrus, CA1–CA3 regions and all layers of the cerebral cortex. Hippocampal sections were photographed at 40× the original magnification, and the cerebral cortex and striatal sections were photographed at 100× the original magnification.

enzyme activity (39) in the brains of Tg2576 mice. Increased levels of a lipid peroxidation product have been noted in Tg2576 mice at ages preceding the appearance of Aβ plaques (38), consistent with the early onset of gene expression changes noted here. A study of cytochrome oxidase activity in another APP over-expressing mouse line examined mice that were old enough to have Aβ plaques (39). However, the quantitation of this marker compared enzyme activity in plaque-free regions, and they found increased levels of Aβ plaques in APP23 mice compared with those in WT mice.

Regardless of the internal consistency of our results, and the consistency between our results and those in the AD literature, our results appear paradoxical: Why would a mouse model of AD, a disease characterized by impaired energy metabolism in the brain (40–46), be associated with the up-regulation of mitochondrial genes? The concomitant up-regulation of genes associated with oxidative damage suggests that the up-regulation of mitochondrial genes is either deleterious itself or is compensatory for an APP-associated insult to the mitochondria—an insult that promotes oxidative damage. The co-localization of ATPase-6 and 8-OHG supports the latter possibility in a compelling way (Fig. 7). From the data in Figure 7, we cannot distinguish whether increased mitochondrial gene expression promotes oxidative damage or whether mitochondrial dysfunction produces both oxidative damage and the up-regulation of the mitochondrial genome. From these data, we also cannot distinguish whether mitochondrial gene expression differences are due to APP, Aβ species or some other product from the mutant human APP over-expression.

In vitro studies of Aβ, however, support the hypothesis that Aβ causes mitochondrial dysfunction. For example, Casley *et al.* (47) incubated rat mitochondria with Aβ, or with Aβ and nitric oxide (which is known to be elevated in the brain of AD patients). They found that Aβ caused a significant reduction in states 3 and 4 of mitochondrial respiration and

Downloaded from https://academic.oup.com/hmg/article/13/12/1225/587912 by guest on 16 August 2022

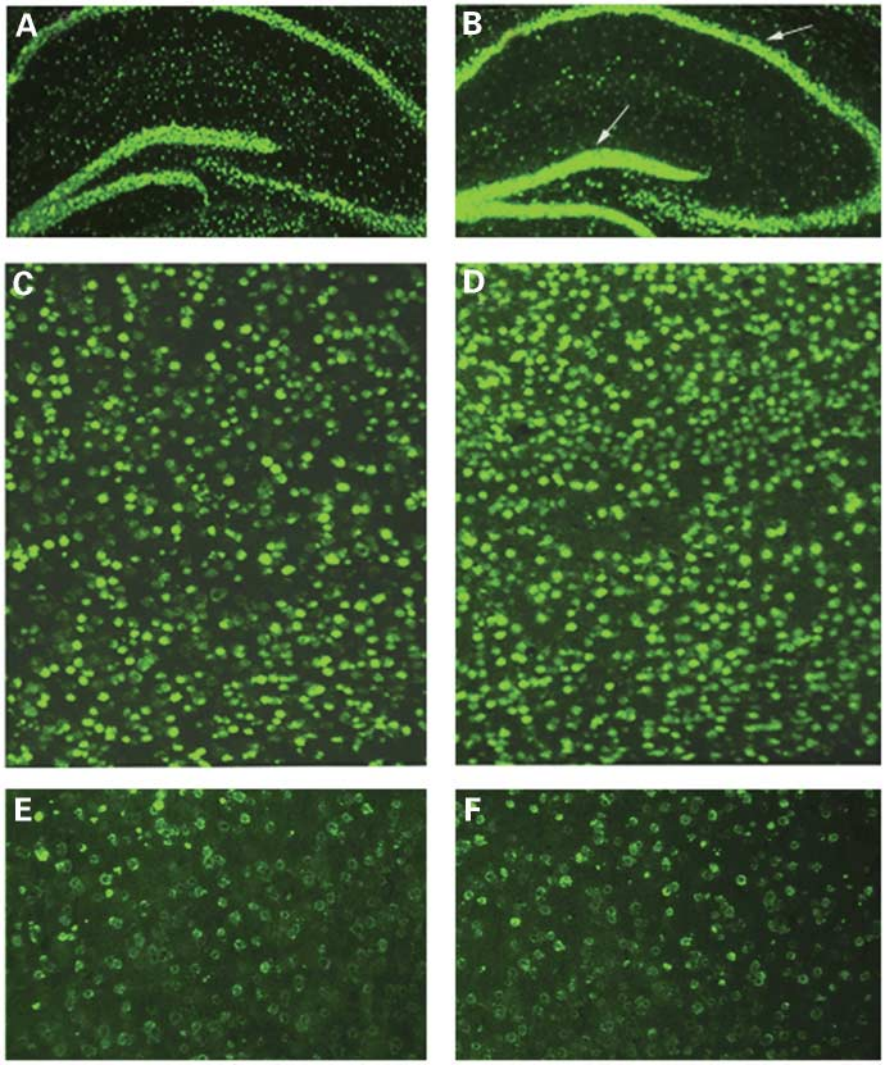

Figure 5. *In situ* hybridization of heat-shock protein 86. Increased mRNA expression of heat-shock protein 86 in green fluorescence is shown in the hippocampus (**A**) and the cerebral cortex (**C**) of age-matched WT mouse compared with sections from the hippocampus (**B**) and the cerebral cortex (**D**) sections of 7-month-old Tg2576 mice. mRNA expression is unchanged for the striatum between Tg2576 mice (**F**) and age-matched WT mice (**E**). Arrows indicate the over-expressions of heat-shock protein 86 in dentate gyrus, CA1–CA3 regions and all layers of the cerebral cortex. Hippocampal sections were photographed at 40× the original magnification, and the cerebral cortex and striatal sections were photographed at 100× the original magnification.

that mitochondrial respiration was further diminished by the addition of nitric oxide. They also found that Aβ inhibited cytochrome oxidase, alpha ketoglutarate dehydrogenase and pyruvate dehydrogenase activities (47).

Even in the face of compelling evidence that mitochondrial gene expression change is due to the expression of mutant APP in multiple experimental models, it remains unclear whether this phenomenon is relevant to AD in humans. Abundant evidence implicates mitochondrial dysfunction in AD, but studies on post-mortem human brains from patients with AD typically find a down-regulation of mitochondrial markers (34). Several studies have reported gene expressions in the brain specimens from AD patients and age-matched control subjects (34,48–56), but such studies of the post-mortem human brain are limited for at least two reasons: (1) there is a significant patient-to-patient variability in mRNA expression due to the heterogeneous genetic make-up of the patient and the control populations and (2) there is a lack of presymptomatic AD brains. Each of these methodological problems can be surmounted by the use of an appropriate animal model, but the generalizability of results to the development of AD in humans is uncertain.

If the Tg2576 mouse model represents very early events in the pathogenesis of AD, however, then the present results may indicate very early and potentially treatable events in human AD. The results from our *in situ* hybridization of ATPase-6, programmed cell death gene 8 and heat-shock protein 86 suggest that neurons in the affected regions of the brain, such as hippocampus and the cerebral cortex, are up-regulated (Figs 3–5), but not in the unaffected regions such as the striatum in Tg2576 mice compared with age-matched WT mice (Figs 3–5). The results from our double-labeling *in situ* hybridization of mitochondrial genes and ATPase-6, and from our immunofluorescence analysis of 8-OHG, which is

Downloaded from https://academic.oup.com/hmg/article/13/12/1225/587912 by guest on 16 August 2022

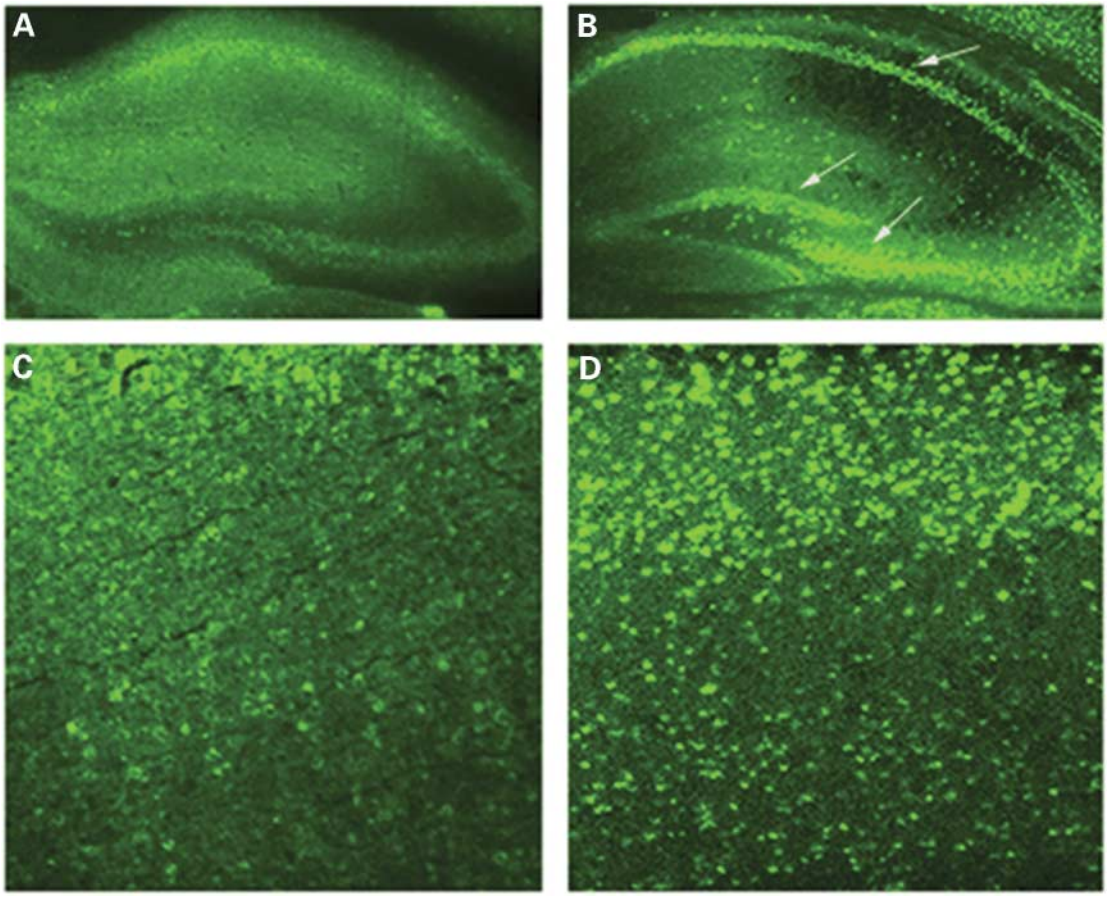

Figure 6. Immunoreactivity with anti-8-OHG. Increased 8-OHG is shown in the hippocampus (**A**) and the cerebral cortex of age-matched WT mice (**C**) compared with sections from the hippocampus (**B**) and the cerebral cortex (**D**) sections of APP mice. Arrows indicate the over-expressions of 8-OHG. Hippocampal sections were photographed at 40× the original magnification, and the cerebral cortex sections were photographed at 100× the original magnification.

a marker of oxidative damage, suggest that only certain over-expressed neurons with ATPase-6 undergo oxidative damage in Tg2576 mice.

This mitochondrial hypothesis is also supported by two independent studies of early AD in human brain tissue. In the first, our laboratory investigated mRNA expression using quantitative real-time PCR to study 11 mitochondrial-encoded genes responsible for OXPHOS in the brain specimens of early AD and definite AD patients (57). We found increased mRNA expressions of subunits in complexes III and IV in the brain specimens of both early and definite AD patients. We also found that the up-regulation of cytochrome oxidase co-localizes with a marker of oxidative damage in human cortical neurons. To determine the role of mitochondrial abnormalities in AD, using *in situ* hybridization, electron microscopy and immuno-histochemistry techniques, Hirai *et al.* studied post-mortem brain specimens from AD patients and control subjects (58). They found that increased oxidative damage in AD patients has a striking and significant increase in mtDNA in pyramidal neurons and cytochrome oxidase in the neuronal cytoplasm indicating that the over-expression of mitochondrial RNA may be the result of an excess of mitochondrial DNA replicating (59) selectively in neurons that undergo oxidative damage. Further, Hirai *et al.* found that the increase in mtDNA and mitochondrial protein in the human AD brain was due to the accumulation of products from degraded mitochondria (ultrastructurally, the mtDNA and the protein were found in cytoplasmic lipofuscin granules), and not due to an increase in morphologically normal mitochondria. Similar to these human mitochondrial data, we found increased mRNA and DNA damage in the neurons of Tg2576 mice (Fig. 7A–C), suggesting that abnormal mitochondrial gene expressions in Tg2576 mice are relevant to AD.

Further, the studies of Hirai *et al.* (58) suggest that the association between mitochondrial abnormalities and oxidative damage is an early event in AD progression in AD patients. These findings are in agreement with our results on Tg2576 transgenic mice. Additional studies are underway to determine the specific molecular species responsible for changes in gene expression and to determine whether these changes can be modified by therapeutic strategies aimed at enhancing mitochondrial function.

On the basis of our gene expression investigations, we propose a model (Fig. 8) in which the over-expressed mutant APP and/or the soluble or insoluble Aβ cause energy deficits selectively in the hippocampus and in the cerebral cortex tissues of APP mice. To compensate for the decreased energy caused by a mutant APP or by soluble and insoluble

Downloaded from https://academic.oup.com/hmg/article/13/12/1225/587912 by guest on 16 August 2022

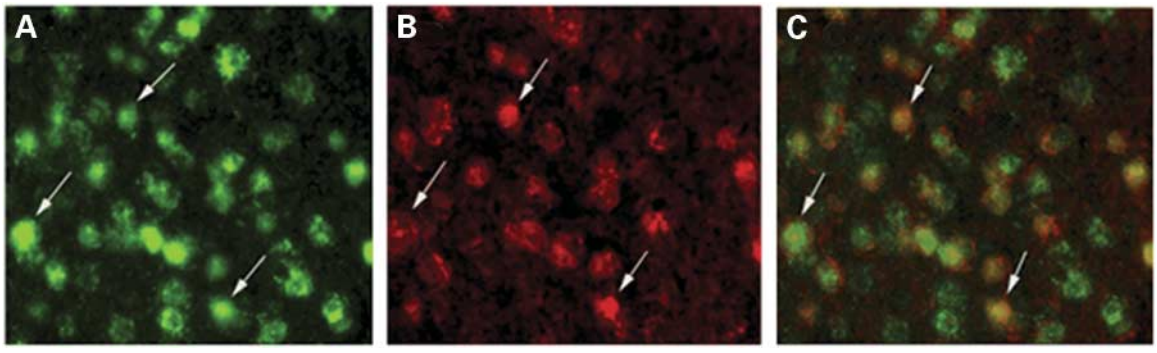

Figure 7. Double-labeling *in situ* hybridization of the mitochondrial gene ATPase-6 and immunofluorescence analysis of 8-OHG from 7-month-old Tg2576 mice. (**A**) ATPase-6 mRNA expression in the cerebral cortex of APP mice. (**B**) 8-OHG immunoreactivity of the same section labeled with ATP-6. (**C**) The overlay of both ATPase-6 and 8-OHG immunoreactivities from the same section. Arrows indicate expressions of ATPase-6 and 8-OHG.

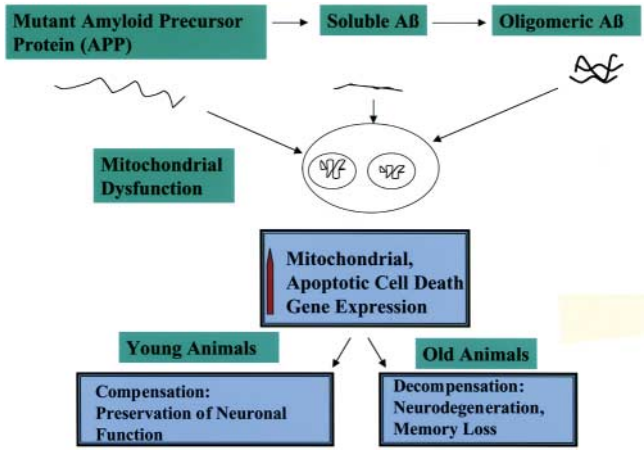

Figure 8. A proposed model of AD pathogenesis in Tg2576 mice. In this model, we propose that over-expressed mutant APP, and/or the soluble or insoluble Aβ probably in the form of monomers and oligomers cause energy deficits selectively in the hippocampus and in the cerebral cortex tissues of Tg2576 mice. To compensate for the decreased energy caused by a mutant APP or by the soluble and/or insoluble Aβ, mitochondrial genes are activated early in AD disease progression in Tg2576 mice. The imbalance between decreased energy metabolism and compensation of energy deficits by the up-regulation of mitochondrial genes may lead to further cellular changes in the late stages of AD progression. The abnormal expressions of mitochondrial genes and their effects on cellular pathways may be ultimately responsible for memory deficits and the neurodegeneration of AD.

Aβ, we hypothesize that mitochondrial genes are activated early in the progression of AD in Tg2576 mice. The imbalance between decreased energy metabolism and compensation of energy deficits by the up-regulation of mitochondrial genes may lead to further cellular changes in the late stages of AD progression. These abnormal expressions of mitochondrial genes and their effects on cellular pathways may be responsible ultimately for memory deficits and neurodegeneration in aged Tg2576 mice.

CONCLUSIONS

We investigated the gene expression profiles of transcripts at three stages of disease progression: long before (2 months), immediately before (5 months) and after (18 months) the appearance of Aβ plaque pathology and cognitive impairment in Tg2576 mice and age-matched WT mice. The gene expression profiles in Tg2576 mice were distinguished by the up-regulation of genes related to mitochondrial energy metabolism and apoptosis in comparison with the corresponding gene expression in age-matched WT mice. This difference was evident in Tg2576 mice by 2 months of age and increased in later stages (5 and 18 months of age) of disease progression. Further, using *in situ* hybridization analysis of the mitochondrial-encoded gene, ATPase-6, programmed cell death gene 8 and heat-shock protein 86, we found that pyramidal neurons in brain slices from the hippocampus and the cerebral cortex are up-regulated in Tg2576 mice compared with those from age-matched WT mice. In addition, the results from our double-labeling *in situ* hybridization of mitochondrial genes and ATPase-6, and our immunofluorescence analysis of 8-OHG (a marker of oxidative damage) suggest that only selectively over-expressed neurons with ATPase-6 undergo oxidative damage in Tg2576 mice. On the basis of findings, we hypothesize that mitochondrial energy metabolism is impaired by the expression of mutant APP and/or Aβ, and that the up-regulation of mitochondrial genes represents a compensatory response. The findings reported here have important implications for the mechanism of Aβ toxicity in AD and for the development of therapeutic strategies.

MATERIALS AND METHODS

An age-matched experimental design was used to examine the gene expression profile of Tg2576 mice at three different stages of disease progression with WT mice (Fig. 9).

Mice

Tg2576 transgenic mice and age-matched WT mice were housed at the Neurological Sciences Institute at the Oregon Health and Science University and at the Veteran Affairs Medical Center. The mice were a generous gift from Dr Karen Hsiao, University of Minnesota. This model was generated with the mutant human APP gene 695 amino acid isoform and with a double mutation ($Lys^{670} \rightarrow Asn$ and

Downloaded from https://academic.oup.com/hmg/article/13/12/1225/587912 by guest on 16 August 2022

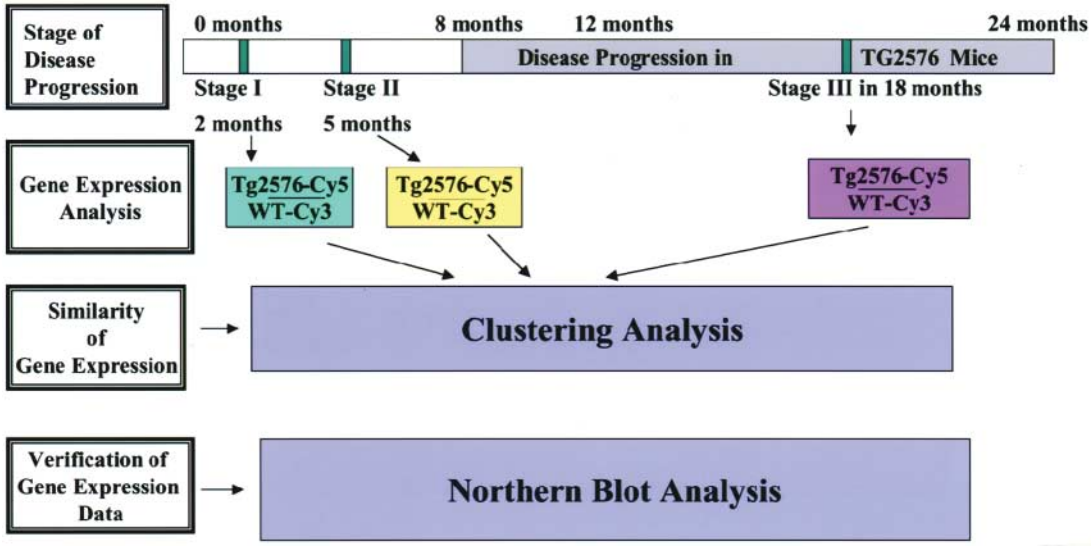

Figure 9. The experimental design, analysis and validation of gene expression data at three stages of disease progression in Tg2576 mice compared with age-matched WT mice.

Met ^{671} → Leu) (11). This highly expressed transgenic line exhibits Aβ plaques, a 5-fold increase in Aβ (1–40) and a 14-fold increase in Aβ (1–42/43) (11). In addition, a correlation has been found between this mouse line and elevated amounts of Aβ formation, and between this mouse line and increased learning and memory deficits (11). These mice mimic AD in the age-dependence appearance of Aβ plaque as well as in the distribution of the Aβ plaque, which is confined to the cerebral cortex and the hippocampus, sparing the striatum, the deep gray nuclei, and the brain stem (11). This mouse model also parallels AD in that the Aβ plaques evoke a microglial reaction in their immediate vicinity (60). However, similar to other transgenic models (12–16,61), this APP mouse model lacks the AD hallmarks of neurofibrillary tangles and neuronal death.

Both Tg2576 mice and age-matched WT mice were sacrificed at 2, 5 and 18 months of age, and the cerebral cortices and the cerebellum tissues were dissected and removed immediately to dry ice and stored at −80°C until the tissue was processed. For each time point, we investigated gene expressions in the cerebral cortex in both Tg2576 mice and age-matched WT mice. We pooled RNA from five Tg2576 mice and five age-matched WT mice for microarray analysis. Prior to the gene expression study of Tg2576 mice and WT mice, we independently examined animal-to-animal biological variability using four WT mice at 2 months of age. The assessment of biological variability is critical when drawing inferences about the gene expression changes of individual animals, based on the results from the pooled sample analysis.

Tissue and RNA preparation

Total RNA was isolated from the cerebral cortices and the cerebellar tissues from Tg2576 mice and WT mice using an RNAeasy kit from Qiagen (Valencia, CA, USA). Briefly, 30–50 mg of tissue was lysed with lysis buffer and homogenized using a rotor–stator homogenizer. An aliquot 600 μl 70% ethanol was added to the homogenate, and samples were then applied to an RNAeasy minispin column for the total RNA to bind to the resin in the column. Total RNA was eluted in 30 μl of RNase-free-water. The RNA concentration was measured for each sample using a spectrophotometer at an absorbance ratio of 260/280 nm. RNA samples were treated with DNA-free DNAse to remove any residual genomic DNA contamination.

Preparation of microarrays

The Spotted Microarray core of the Gene Microarray Shared Resource at Oregon Health and Science University obtained ∼15 000 cDNA clones from the NIA (NIH, Baltimore, MD, USA). Based on clones, cDNAs were re-arrayed from 52 374 ESTs—originally cloned ESTs prepared from RNA from E12.5 female gonad/mesonephors and new-born baby. These clones are associated functionally with several cellular pathways, including matrix and structural proteins, energy metabolism, transcription factors, protein synthesis, translational control, signal transduction, heat-shock and stress-related genes (62,63). The embryonically expressed clones were good candidates for our gene expression investigations because our proposed study was primarily interested in genes related to early cellular events in AD disease progression. Based on this library, the microarray core created two high-density cDNA chips containing a total of 11 283 cDNAs. The cDNA clones were sequence-verified and represented the 3′ end of the gene from the mouse (62,63). The core used a duplicate half-slide (i.e. each gene had duplicate spots on the same slide) and duplicate slides to reduce intra-slide and inter-slide technical variability. This method produced four signal values from each gene that were averaged after pre-processing and normalization (see later).

Downloaded from https://academic.oup.com/hmg/article/13/12/1225/587912 by guest on 16 August 2022

Labeling of RNA and hybridization of microarrays

For the hybridization of RNA in each slide, we used 4.5 μg of total RNA. We labeled the RNA using the method described by Karsten *et al.* (64), but slightly modified. The Perkin–Elmer TSA kit was used for visualization of the hybridized target cDNA. Briefly, polyadenylated RNA was reverse-transcribed using an oligo-dT primer. Fluorescein-modified or biotinylated nucleotides were incorporated into the extending strand. After removal of the unincorporated nucleotides from the mix using Amicon YM100 spin cups, the target cDNA mix was hybridized to an appropriate array for 16 h at 65°C. The hybridized arrays were washed in 0.06 × SSC, blocked using a proprietary blocking agent in Tris–saline with added goat serum and then incubated with anti-fluorescein antibodies linked to horseradish peroxidase (HRP). After being washed to remove the excess Ab–HRP, the slides were incubated with a Cy3-tyramine derivative to produce a Cy3 product at the site of hybridization. The HRP became completely inactivated. The hybridized arrays were then incubated with streptavidin-linked HRP, followed by a treatment of Cy5-linked tyramine, resulting in a Cy5 product at the site of hybridization.

Dried, hybridized arrays were scanned with a Perkin–Elmer ScanArray 4000XL and stored as 16-bit TIFF files. These files were gridded and quantified using the array analysis software ImaGene® (BioDiscovery, El Segundo, CA, USA). The output file contained the mean value of each spot, the mean value for the local background, the standard deviation for both measures and a number of user-selected quality control measures.

Microarray data pre-processing and normalization

We computed the background-adjusted signal intensities by subtracting the mean local background intensity from the mean signal intensity. Negatively adjusted signals were flagged and removed from subsequent analysis. The data were filtered using a threshold value based on the 95th percentile of blank spots. For each gene, there were four technical replicates. Any genes with expression values below this threshold for any of the four technical replicates were considered absent or not expressed, and were not included for further analysis. Normalization was performed using the within-slide, intensity-dependent normalization method of Yang *et al.* (65). To address the issue of outlier detection, any gene with an absolute value of studentized residual >2 or Cook's distance >2 for any of the four technical replicates was marked as an outlier and filtered out ('$N = 4$ filter'). Data were required to pass the $N = 4$ filter in all time points to be included in the analysis. Based on these criteria, 4779 genes were selected for further study. Normalized gene expression values are reported as log 2, ratios denoted as NLR.

Assessment of animal–animal biological variability

To examine animal–animal biological variability of gene expression before pooling RNA, we used RNA prepared from the cerebral cortices of four WT mice and labeled them with Cy3. The universal mouse reference RNA from Stratagene was used as a common reference and labeled with Cy5. The correlation coefficients of a filtered normalized log ratio (NLR) ranged from 0.87 to 0.91, indicating relatively high reproducibility of gene expression profiles among individual animals (Supplementary Material, Fig. S1).

Visualization and selection of genes

4779 genes that passed the $N = 4$ filter at each of the three time points were then examined by hierarchical cluster analysis. Owing to the age-matched design of the study, clustering was seen mainly as a descriptive tool to aid in visualizing the data set and to aid us in selecting genes for confirmation studies. The genes were annotated with the gene ontology functions for biological processes, molecular functions and cellular compartments to allow the rapid identification of genes with similar gene expression patterns and functional roles. Based on this annotation, one of the clusters was quickly identified by a high concentration of mitochondrial genes with the highest average mRNA fold change (average FC = 2.8). Several representative genes from this cluster were selected for further validation via northern blot analysis.

Validation of microarray data—northern blot analysis

To validate cDNA microarray results, using Northern blot analysis, we measured mRNA expressions in the cerebral cortex and cerebellum of both Tg2576 mice and age-matched WT mice in 18 representative differentially expressed genes at the three stages of AD progression, from the highest average mRNA fold change: mt gene–NADH subunit 1 (complex I), mt gene–NADH subunit 2 (complex I), mt gene–NADH subunit 3 (complex I), mt gene–NADH subunit 4 (complex I), mt gene–NADH subunit 5 (complex I), mt gene–NADH subunit 6 (complex I), mt gene–cytochrome *b* (complex III), mt gene–cytochrome-*c*-oxidase subunit 1 (complex IV), mt gene–cytochrome-*c*-oxidase subunit 2 (complex IV), mt gene–cytochrome-*c*-oxidase subunit 3 (complex IV), mt gene–ATPase-6 (complex V), chemokine receptor 4 (CXCR 4), programmed cell death gene 8, nexin 14, tripeptidyl peptidase, heat-shock protein 86 and alpha-tubulin. To determine whether RNA expression changes are confined to only the affected region in Tg2576 mice, we also studied the cerebellum of both Tg2576 mice and WT mice for the same genes studied for the cerebral cortex.

The cDNA clones were purchased from ATCC (Manassas, VA, USA). They represent 3′ regions of both translated and untranslated regions of cDNAs. They were grown in Lunia–Bertani broth containing an appropriate antibiotic for plasmid DNA preparation, and they were verified for their originality and their entirety. cDNA inserts were released by restriction digest analysis using appropriate restriction enzymes. The cDNA inserts were electrophoresed on a low-melt agarose gel, purified using a Promega DNA purification kit (Madison, WI, USA) and then used as a probe in northern blot analysis.

Total RNA was extracted from the brains of Tg2576 mice and WT mice using either the TRIzol reagent (Life Technologies, Inc., Gaithersburg, MD, USA) or an RNA easy kit (Qiagen). For northern blot analysis, we prepared RNA from APP and WT mice (at the same three time points as we used in our microarray studies but from different mice). An amount of 5 μg of total RNA was size-fractionated on 1%

Downloaded from https://academic.oup.com/hmg/article/13/12/1225/587912 by guest on 16 August 2022

agarose gel using standard northern blot reagents and conditions. The RNAs were transferred onto nylon membranes. About 100 ng of cDNA insert was labeled with ^{32}P α-dCTP (Amersham Pharmacia, Inc., Piscataway, NJ, USA). The membranes were pre-hybridized with a 50% de-ionized formamide buffer for 2–3 h at 55°C. Then the membranes were hybridized overnight with a radio-labeled probe, were washed at room temperature and at 42°C and exposed to X-ray film for 30 min to overnight at −80°C. The bands in the northern blot analysis were scanned on a Kodak scanner (ID Image Analysis Software, Kodak Digital Science, Kennesaw, GA, USA). The lanes were marked to define the position and specified regions of the bands. Then the ID fine-band command was used to locate the bands in each lane. The bands were scanned, and the readings were recorded.

In situ hybridization of mitochondrial and oxidative damage-related genes in Tg2576 mice and age-matched WT mice

To determine the localization of the most up-regulated genes, including mitochondrial-encoded ATPase-6 in complex V, programmed cell death gene 8 and heat-shock protein 86, using *in situ* hybridization techniques, we studied ATPase-6, programmed cell death gene 8 and heat-shock protein 86 in the brain specimens of 7-month-old Tg2576 mice ($n = 5$) and age-matched WT mice ($n = 5$).

The mice were sacrificed by cervical dislocation, and their brains were quickly dissected, frozen in TissueTek (VWR Scientific, West Chester, PA, USA) and stored at −80°C. We cut 10–15 μm-thick coronal sections, thaw-mounted them on superfrost slides (Fisher Scientific, Pittsburgh, PA, USA) and stored them at −80°C until use. cDNA clones of mitochondrial-encoded ATPase-6, programmed cell death gene 8 and heat-shock protein 86 were purchased from ATCC (Manassas). At the time of purchase, these cDNAs were already subcloned into expression vectors containing SP6 and T7 promoters for RNA polymerases.

DIG-RNA probes were transcribed from plasmid cDNA inserts. The orientation of these cDNA clones were as follows: 5′ end of the gene towards the T7 side and 3′ end of the gene towards the SP6 or T3 side of the vector. The template DNAs were linearized for *in vitro* transcription so that SP6/T3 and T7 RNA polymerases generated the anti-sense and sense strands. In 20 μl of reaction, 1 μg of a linearized template DNA was labeled with 40 U of SP6 (for the anti-sense strand) and 40 U of T7 (for the sense strand) RNA polymerase, 2 μl of 100 mM dithiothreitol (DTT), 2 μl of DIG-dNTPS, 4 μl of 5 × transcription buffer (Promega) and 20 U of RNAse inhibitor. These substances constituted the total volume up to 20 μl with DPEC·H_2O. The contents were incubated for 2 h at 37°C.

Frozen cut brain sections (15 μ thick) from Tg2576 mice and WT mice were fixed for 2 h in a fresh 4% *para*formaldehyde after thawing the sections at room temperature. The sections were washed three times with phosphate-buffered saline (PBS) (pH 7.4) 3 min each, and two times with 2× SSPE buffer. The sections were hybridized for 1 h with a prehybridization buffer [containing 50% formamide, 2× SSPE, t-RNA 2 μg/μl, (BSA) 1 μg/μl, poly A 0.5 μg/μl and 10 mM DTT] and hybridized overnight at 60°C with a hybridization buffer plus gene specific *in vitro*-transcribed ribo-probe 2 μg/ml. The sections were washed three times with 2× SSPE buffer for 15 min each, and once with 1× SSPE at 60°C. Then the sections were washed once with PBS (pH 7.4) and blocked for 30 min at room temperature with 1% blocking buffer (Molecular Probes). The sections were treated with a sheep anti-DIG polyclonal antibody for 1 h, washed three times with PBS (pH 7.4), then treated with the fluorescent dye Alexa 488 (green color, Molecular Probes) for 10 min at room temperature and counter-stained with Hoechst (1:1000, blue color) for nuclear labeling.

Immunofluorescence analysis of mitochondrial and oxidative damage-related genes in the brain specimens of Tg2576 mice and age-matched WT mice

To determine the relationship between mitochondrial gene up-regulation and oxidative damage, we also studied 8-OHG, a marker for oxidative damage, in 7-month-old Tg2576 mice ($n = 5$) and age-matched WT mice ($n = 5$) brain specimens.

Frozen cut brain sections (15 μm thick) from Tg2576 mice and WT mice were fixed for 2 h in a fresh 4% *para*formaldehyde after allowing sections to reach room temperature. To block the endogenous peroxidase, sections were treated for 30 min with H_2O_2 and then with 0.5% Triton X dissolved in PBS pH 7.4. The sections were blocked with a solution (0.5% Triton X in PBS + 10% rabbit serum +1% BSA) and then incubated overnight at room temperature with a goat anti-8-OHG, polyclonal antibody (1:50 dilution, Alpha Diagnostics, San Antonio, TX, USA). On the day after primary antibody incubation, the sections were washed with a washing buffer (0.5% Triton X in PBS).

For 8-OHG, the sections were incubated with a secondary biotinylated anti-mouse antibody, 1:2000 (Vector Laboratories, Burlingame, CA, USA) for 1 h at room temperature. Sections were washed with PBS (pH 7.4) three times for 10 min each. They were blocked for 1 h with 1% blocking buffer (Molecular Probes) and then incubated with the labeled streptavidin–HRP (SA–HRP) solution for 1 h (Molecular Probes). The sections were washed with PBS (pH 7.4) three times each for 10 min, then treated with the fluorescent dye Alexa 488 (green color, Molecular Probes) for 10 min at room temperature and counter-stained with Hoechst (1:1000, blue color) for nuclear labeling. Photographs were taken using a confocal microscope.

Double-labeling analysis of ATPase-6 and 8-OHG in the brain specimens of Tg2576 mice and age-matched WT mice

To determine whether neurons showing increased ATPase-6 expression are more vulnerable to oxidative damage, we conducted double-labeling, a combination *in situ* hybridization for the mitochondrial gene ATPase-6, using ATPase-6 riboprobe, and immunofluorescence analysis for 8-OHG, using goat anti-8-OHG antibody (Alpha Diagnostics).

For the first labeling, the sections were fixed in 4% *para*-formaldehyde and hybridized overnight at room temperature with DIG-ATPase-6 riboprobe (1 μg/ml). On the next day, the sections were incubated with an anti-DIG antibody

Downloaded from https://academic.oup.com/hmg/article/13/12/1225/587912 by guest on 16 August 2022

(Roche Diagnostics, Indianapolis, IN, USA) in a dilution 1:200 for 1 h at room temperature and then treated with the fluorescent dye Alexa 488 (green color, molecular Probes) for 10 min at room temperature.

For the second labeling, the sections were treated with 3% H_2O_2 blocked with 10% rabbit serum and then incubated overnight with a primary goat anti-OHG polyclonal antibody (1:50 dilution Alpha Diagnostics). On the third day, slides were incubated with a secondary biotinylated rabbit anti-goat antibody in a 1:500 dilution (Vector Laboratories) for 1 h at room temperature and then incubated with SA–HRP in a 1:100 dilution for 1 h at room temperature (Molecular Probes). Finally, the slides were incubated with the fluorescent dye Alexa 594 (red color). Photographs were taken with a confocal microscope.

SUPPLEMENTARY MATERIAL

Supplementary Material is available at HMG Online.

ACKNOWLEDGEMENTS

The authors thank Sandra Oster, Neurological Sciences Institute, Oregon Health and Science University, for critical reading of the manuscript. This research was supported in part by the Alzheimer's Association of Oregon, the Medical Research Foundation of Oregon, the American Federation for Aging Research, a pilot grant from the Alzheimer's Disease Center of Oregon, P30 AG08017, and AG22643 (to P.H.R.) and Department of Veteran's Affairs Advanced Research Career Development Award and NIH-AT0006 (to J.Q.).

REFERENCES

1. Selkoe, D.J. (2001) Alzheimer's disease: genes, proteins, and therapy. *Physiol. Rev.*, **81**, 741.
2. Tanzi, R.E. and Bertram, L. (2001) New frontiers in Alzheimer's disease genetics. *Neuron*, **32**, 181–184.
3. Holmes, C. (2002) Genotype and phenotypes in Alzheimer's disease. *Br. J. Psychiatry*, **180**, 131–134.
4. Hardy, J. and Selkoe, D.J. (2002) The amyloid hypothesis of Alzheimer's disease: progress and problems on the road to therapeutics. *Science*, **297**, 353–356.
5. Terry, R.D., Masliah, E. and Hansen, L.A (1991) The neuropathology of Alzheimer's disease and the structural basis of cognition alterations. In Terry, R.D., Katzman, R. and Bick, K.l. (eds), *Alzheimer's Disease*. Raven Press, New York, pp. 187–306.
6. Mattson, M.P., Parting, J. and Begley, J.G. (1998) Amyloid beta-peptide induces apoptosis-related events in synapses and dendrites. *Brain. Res.*, **807**, 76–82.
7. Marques, C.A., Keil, U., Bonert, A., Steiner, B., Haass, C., Muller, W.E. and Eckert, A. (2003) Neurotoxic mechanisms caused by the Alzheimer's disease-linked Swedish amyloid precursor protein. *J. Biol. Chem.*, **278**, 28294–28302.
8. Eckert, A., Steiner, B., Marques, C., Leutz, S., Romig, H., Haass, C. and Muller, W.E. (2001) Elevated vulenerability to oxidative-stress induced cell death and activation of caspase 3 by the Swedish amyloid precursor protein mutation. *J. Neurosci. Res.*, **64**, 183–192.
9. Stepahn, A., Laroche, S. and Sabrina, D. (2001) Generation of aggregated β-Amyloid in the rat hippocampus impairs synaptic transmission and plasticity and causes memory deficits. *J. Neurosci.*, **21**, 5703–5714.
10. Stepanichev, M.Y., Moiseeva, Y.V., Lazareva, N.A., Onufriev, M.V. and Gulyava, N.V. (2003) Single intracerebroventricular administration of amyloid-beta (25–35) peptide induces impairment in short term rather than long-term memory in rats. *Brain. Res. Bull.*, **61**, 197–205.
11. Hsiao, K., Chapman, P., Nilsen, S., Eckman, C., Harigaya, Y., Younkin, S., Yang, F. and Cole, G. (1996) Correlative memorydeficits. A beta elevation, and amyloid plaques in transgenic mice. *Science*, **274**, 99–102.
12. Duff, K., Eckman, C., Zehr, C., Yu, X., Prada, C.M., Perez-Tur, J., Hutton, M., Buee, L., Harigaya, Y., Yager, D. *et al.* (1996) Increased amyloid- 42(43) in brains of mice expressing mutant presenilin 1. *Nature*, **383**, 710–713.
13. Games, D., Adams, D., Alessandrini, R., Barbour, R., Berthelette, P., Blackwell, C., Carr, T., Clements J., Donaldson, T. and Gillespie, F. (1997) Alzheimer-type neuropathology in transgenic mice over expressing V717F β amyloid precursor protein. *Nature*, **373**, 523–527.
14. Borchelt, D.R., Ratovitsky, T., van Lare, J., Lee, M.K., Gonzales, V., Jenkins, N.A., Copeland, N.G., Price, D.L. and Sisodia, S.S. (1997) Accelerated amyloid deposition in the brains of transgenic mice coexpressing mutant presenilin 1 and amyloid precursor proteins. *Neuron*, **19**, 939–945.
15. Lamb, B.T., Call, L.M., Slunt, H.H., Bardel, K.A., Lawler, A.M., Eckman, C.B., Younkin, S.G., Holt, G, Wagner, L., Price, D.L. *et al.* (1997) Altered metabolism of familial Alzheimer's disease-linked amyloid precursor protein variants in yeast artificial chromosome transgenic mice. *Hum. Mol. Genet.*, **6**, 1535–1541.
16. Lamb, B.T., Bardel, K.A., Kulnane, L.S. anderson, J.J., Holtz, G., Wagner, S.L., Sisodia, S.S. and Hoeger, E.J. (1999) Amyloid production and deposition in mutant amyloid precursor protein and presenilin-1 yeast artificial chromosome transgenic mice. *Nat. Neurosci*, **2**, 695–697.
17. Odde, S., Caccamo, A., Sheperd, J.D., Murphy, M.P., Golde, T.E., Kayed, R., Metherate, R., Mattson, M.P., Akbari, Y. and LaFerla, F.M. (2003) Triple transgenic model of Alzheimer's Disease with plaques and tangles: intracellular Aβ and synaptic dysfunction. *Neuron*, **39**, 409–421.
18. Kawarabayashi, T., Younkin, L.H., Saido, T.C., Shoji, M., Ashe, K.H. and Younkin, S.G. (2001) Age-dependent changes in brain, CSF, and plasma amyloid (beta) protein in the Tg2576 transgenic mouse model of Alzheimer's disease. *J. Neurosci.*, **21**, 372–381.
19. Westerman, M.A., Cooper-Blacketer, D., Mariash, A., Kotilinek, L., Kawarabayashi, T., Younkin, L.H., Carlson, G.A., Younkin, S.G. and Ashe, K.H. (2002) The relationship between Abeta and memory in the Tg2576 mouse model of Alzheimer's disease. *J. Neurosci.*, **22**, 1858–1867.
20. Stackman, R.W., Eckenstein, F., Frei, B., Kulhanek, D., Nowlin, J. and Quinn, J.F. (2003) Prevention of age-related spatial memory deficits in a transgenic mouse model of Alzheimer's disease by chronic *Ginkgo biloba* treatment. *Exp. Neurol*, **184**, 510–520.
21. Jantaranotai, N., Ryu, J.K., Kim, S.U. and McLarnon, J.G. (2003) Amyloid beta peptide-induced corpus callosum damage and glial activation *in vivo. Neuro. Rep.*, **14**, 1429–1433.
22. Mucke, L., Masliah, E., Yu, G.-Q., Mallory, M., Rockenstein, E.M., Tatsuno, G., Hu, K., Kholodenko, D., Johnson-Wood, K. and McConglogue L. (2000) High-level neuronal expression of abeta 1-42 in wild type human amyloid precursor transgenic mice: synaptotoxicity without plaque formation. *J. Neurosci.*, **20**, 4050–4058.
23. Selkoe, D.J. (2002) Alzheimer's disease is a synaptic failure. *Science*, **298**, 789–791.
24. Townsend, K.P., Obregon, D., Quadros, A., Patel, N., Volmar, C.H., Paris, D. and Mullan, M. (2002) Proinflammatory and vasoactive effects of Abeta in the cerebrovasculature. *Ann. NY, Acad. Sci.*, **977**, 65–76.
25. Paris, D., Humphrey, J., Quadros, A., Patel, N., Crescentini, R., Crawford, F. and Mullan. M. (2003) Vasoactive effects of A beta in isolated human cerebrovessels and in a transgenic mouse model of Alzheimer's disease: role of inflammation. *Neurol. Res.*, **25**, 642–651.
26. Lehman, E.H., Kulnane, L.S. and Lamb, B.T. (2003) Alterations in β-amyloid production and deposition in brain regions of two transgenic models. *Neurobiol. Aging.*, **24**, 645–653.
27. Irizarry, M.B., Locascio, J.L. and Hyman, B.T. (2001) β-Site APP cleaving enzyme mRNA expression in APP transgenic mice: anatomical overlap with transgene expression and static levels with aging. *Am. J. Pathol.*, **158**, 173–177.
28. The Gene Ontology Consortium. (2000) Gene Ontology: tool for the unification of biology. *Nat. Genet.*, **25**, 25–29.
29. The Gene Ontology Consortium. (2001) Creating the gene ontology resource: design and implementation. *Genome Res.*, **11**, 1425–1433.

Downloaded from https://academic.oup.com/hmg/article/13/12/1225/587912 by guest on 16 August 2022

30. Hill, D.P., Blake, J.A., Richardson, J.E. and Ringwald, M. (2002) Extension and integration of the Gene Ontology (GO): combining GO vocabularies with external vocabularies. *Genome Res.*, **12**, 1982–1991.
31. The Gene Ontology Consortium. (2004) The Gene Ontology (GO) database and informatics resource. *Nucl. Acids Res.*, **32**, D258–D261.
32. Sreedhar, A.S. and Csermely, P. (2004) Heat shock proteins in the regulation of apoptosis: new strategies in tumor therapy: a comprehensive review. *Pharmacol. Ther.*, **101**, 227–257.
33. Gregori, L., Hainfeld, J.F., Simon, M.N. and Goldgaber, D. (1997) Binding of amyloid beta protein to the 20S proteasome. *J. Biol. Chem.*, **272**, 58–62.
34. Loring, J.F., Wen, X., Lee, J.M., Seilhamer, J. and Somogyi, R. (2001) A gene expression profile of Alzheimer's disease. DNA. *Cell. Biol.*, **20**, 682–695.
35. Stein, T.D. and Johnson, J.A. (2002) Lack of neurodegeneration in transgenic mice overexpressing mutant amyloidprecursor protein is associated with increased levels of transthyretin and the activation of cell survival pathways. *J. Neurosci.*, **22**, 7380–7388.
36. Dickey, C.A., Loring, J.F., Montogemery, J., Gordon, M.N., Eastman, P.S. and Morgan, D. (2003) Selectively reduced expression of synaptic plasticity-related genes in amyloid precursor protein + presenilin 1 transgenic mice. *J. Neurosci.*, **23**, 5219–5226.
37. Smith, M.A., Hirai, K., Hsiao, K., Papolla, M.A., Harris, P.L., Siedlak, S.L., Tabaton, M. and Perry, G. (1998) Amyloid-betadeposition in Alzheimer transgenic mice is associated with oxidative stress. *J. Neurochem.*, **70**, 2212–2215.
38. Pratico, D., Uryu, K, Leight, S., Trojanowski, J.Q. and Lee, V.M. (2001) Increased lipid peroxidation precedes amyloid plaque formation in an animal model of Alzheimer amyloidosis. *J. Neurosci.*, **21**, 4183–4187.
39. Strazielle, C., Sturchler-Pierrat, C., Staufenbiel, M. and Lalonde, R. (2003) Regional brain cytochrome oxidase activity in beta-amyloid precursor protein transgenic mice with the Swedish mutation. *Neuroscience*, **118**, 1151–1163.
40. Blass, J.P. and Gibson, G.E. (1991) The role of oxidative abnormalities in the pathophysiology of Alzheimer's disease. *RevNeuro*, **147**, 513–525.
41. Blass, J.P. (1993) Metabolic alterations common to neural and non-neural cells in Alzheimer's disease. *Hippocampus*, **3**, 45–54.
42. Blass, J.P. (1997) Cerebral metabolic impairments. In Khachuaturian, Z.S., Radebaugh, T.S. (Eds), *Alzheimer's Disease: Cause(s), Diagnosis, Treatment, and Care*. CRC Press, NY, pp. 187–206.
43. Blass, J.P. (2001) Brain metabolism and brain disease: is metabolic deficiency the proximate cause of Alzheimer dementia? *J. Neurosci. Res.*, **66**, 851–856.
44. Gibson, G.E., Sheu, K.F. and Blass, J.P. (1998) Abnormalities of mitochondrial enzymes in Alzheimer's disease. *J. Neural. Transm.*, **105**, 855–870.
45. Beal, M.F. (1998) Mitochondrial dysfunction in neurodegenerative diseases. *Biochim. Biophys. Acta*, **1366**, 211–213.
46. De la Monte, S.M., Luong, T.L., Neely, T.R., Robinson, D. and Wands, J.R. (2000) Mitochondrial DNA damage as a mechanism of cell loss in Alzheimer's disease. *Lab. Invest.*, **80**, 1323–1335.
47. Casley, C.S., Canevari, L., Land, J.M., Clark, J.B. and Sharpe, M.A. (2002) Beta-amyloid inhibits ntegratedmitochondrial respiration and key enzyme activities. *J. Neurochem.*, **80**, 9–100.
48. Chow, N., Cox, C., Callahan, L.M., Weimer, J.M., Guo, L. and Coleman, P.D. (1998) Expression profiles of multiple genes in single neurons of Alzheimer's disease. *Proc. Natl Acad. Sci. USA*, **95**, 9620–9625.
49. Ginsberg, S.D., Hemby, S.E., Lee, V.M.-Y., Eberwine, J.H. and Trojanowski, J.Q. (2000). Expression profile of transcripts in Alzheimer's disease tangle bearing CA1 neurons. *Ann. Neurol*, **48**, 77–87.
50. Hata, R., Masumura, M., Akatsu, H., Li, F., Fugita, H., Nagai, Y., Yamamoto, T., Okada, H., Kosaka, K., Sakanaka, M. and Sawada, T. (2001) Up-regulation of calcineurin Aβ mRNA in the Alzheimer's disease brain: assessment by cDNA microarray. *Biochem. Biophys. Res. Commun.*, **284**, 310–316.
51. Ho, L., Gou Y., Spielman, L., Petrescu, O., Haroutunian, V., Purohit, D., Czernik, A., Yemul, S., Aisen, P.S. and Mohs, R. (2001) Altered expression of a-type but not b-type synapsin isoform in the brains of patients at high risk for Alzheimer's disease assessed by DNA microarray technique. *Neurosci. Lett.*, **298**, 191–194.
52. Doyu, M., Sawada, K.I., Mitsuma, N., Niwa, J.I., Yahshimoto, M., Fujii, Y., Sobue, G. and Kato, K. (2001) Gene expression profile in Alzheimer's brain screened by molecular indexing. *Mol. Brain Res.*, **87**, 1–11.
53. Colangelo, V., Schurr, J., Ball, M.J., Pelaez, R.P., Bazan, N.G. and Lukiw, W.J. (2002) Gene expression profiling of 12633 genes in Alzheimer hippocampal CA1: transcription and neurotrophic factor down-regulation and up-regulation of apoptotic and pro-inflammatory signaling. *J. Neurosci. Res.*, **70**, 462–473.
54. Mufson, E.J., Counts, S.E. and Ginsbergm S.D. (2002) Gene expression profiles of cholinergic nucleus basalis neurons in Alzheimer's disease. *Neurochem. Res.*, **27**, 1035–1048.
55. Hemby, S.E., Trojanowski, J.Q. and Ginsberg, S.D. (2003) Neuron-specific age-related decreases in dopamine receptor subtype mRNAs. *J. Comput. Neurol.*, **456**, 176–183.
56. Gutala, R.V. and Reddy, P.H. (2004) The use of real-time PCR analysis in a gene expression study of Alzheimer's disease postmortem brain. *J. Neurosci. Meth.*, **132**, 101–107.
57. Manczak, M., Park, B.S., Jung, Y. and Reddy, P.H. (2004) Differential expression of oxidative phosphorylation genes in patients with Alzheimer's disease: implications for early mitochondrial dysfunction and oxidative damage. *NeuroMol. Med.*, **5**, 147–162.
58. Hirai, K., Aliev, G., Nunomura, A., Fujika, H., Russell, R.L., Atwood, C.S., Jophnson, A.B., Kress, Y., Vinters, H.V., Tabaton, M. *et al.* (2001) Mitochondrial abnormalities in Alzheimer's disease. *J. Neurosci.*, **21**, 3017–3023.
59. Fernandez-Silva, P., Enriquez, J.A. and Montoya, J. (2003) Replication and transcription of mammalain mitochondrial DNA. *Exp. Physiol.*, **88.1**, 41–56.
60. Frautschy, S.A., Yang, F., Irrizarry, M., Hyman, B., Saido, T.C., Hsiao, K. and Cole, G.M. (1998) Microglial response to amyloid plaques in APPsw transgenic mice. *Am. J. Pathol.*, **152**, 307–317.
61. Irizarry, M.C., McNamara, M., Fedorchak, K., Hsiao, K. and Hyman, B.T. (1997) APPSw transgenic mice develop age-related A beta deposits and neuropil abnormalities, but no neuronal loss in CA1. *J. Neuropathol. Exp. Neurol.*, **56**, 965–973.
62. Tanaka, T.S., Jaradat, S.A., Lim, M.K., Kargul, G.J., Wang, X., Grahovac, M.J., Pantano, S., Sano, J., Nagaraja, R., Doi, H. *et al.* (2000). Genome-wide expression profiling of mid-gestation placenta and embryo using a 15,000 mouse developmental cDNA microarray. *Proc. Natl Acad. Sci. USA*, **97**, 9127–9132.
63. Kargul, G.J., Dudekula, D.B., Qian, Y., Lim, M.K., Jaradat, S.A., Tanaka, T.S., Carter, M.G. and Ko, M.S. (2001) Verification and initial annotation of the NIA mouse 15K cDNA clone set. *Nat. Genet.*, **28**, 17–18.
64. Karsten, S.L., Van Deerlin, V.M., Sabatti, C., Gill, L.H. and Geschwind, DH. (2002) An evaluation of tyramide signal amplification and archived fixed and frozen tissue in microarray gene expression analysis. *Nucl. Acids Res.*, **30**, E4.
65. Yang, Y.H., Dudoit, S., Liu, P., Lin, D.M., Peng, V., Hgai, J. and Speed, T.P. (2002) Normalization for cDNA microarray data: a robust composite method addressing single and multiple slide systematic variation. *Nucl. Acids Res.*, **30**, E15.

Downloaded from https://academic.oup.com/hmg/article/13/12/1225/587912 by guest on 16 August 2022